

## Emission-Line CCD Imaging of Three Southern Symbiotic Stars

Harish C. Bhatt & Ram Sagar *Indian Institute of Astrophysics, Bangalore*  
560034

Received 1990 December 27; accepted 1991 March 25

**Abstract.** Symbiotic stars that are strong radio sources and have cool dust emitting in the infrared are expected to have extended emission nebulae around them. In order to search for such emission nebulae, we have carried out CCD imaging of three symbiotic stars (R Aqr, RR Tel and H1-36) with narrow-band filters centred at the emission lines of [O III]  $\lambda 5007$ , H $\alpha$   $\lambda 6563$ , [N II]  $\lambda 6584$ , [S II]  $\lambda 6717 + 6731$ . RR Tel and H1-36 images do not show any extended nebulosities around them. The CCD image of the R Aqr nebulosity in the high excitation [O III] line is different from its image in H $\alpha$  and the low excitation lines of [N II] and [S II] indicating ionization-stratification in the nebula. In H1-36 the optical nebulosity (if it exists) is smaller than  $\sim 2$  arcsec while the radio image size is known to be large ( $\sim 5$  arcsec). This behaviour is opposite to that seen in R Aqr in which the radio emission comes from the core region of a much larger optical nebulosity. Interstellar and/or circumstellar extinctions are suggested to be responsible for this difference.

*Key words:* narrow-band CCD imaging—symbiotic star—morphology

### 1. Introduction

Symbiotic stars display spectral features associated with both red giant stars and planetary nebulae. Thus they exhibit the absorption features of a late-type giant star and also emission lines of H $\beta$ , He I and of ions (*e.g.* O $^{++}$ ) with ionization potential  $\geq 20$  eV (see *e.g.* Kenyon 1986). The emission lines are formed in a region of ionized gas around the hot component that is the source of ionizing ultraviolet photons in these systems. This is similar to planetary nebulae. The ionized regions in planetary nebulae are large in extent ( $\geq 10^{16}$  cm) and appear as emission nebulae in optical photographs. At radio frequencies (say 5 GHz) most planetary nebulae are easily detected. Most symbiotic stars on the other hand are not detected at radio wavelengths; and those that are detected, are weak sources. Only a few symbiotics have been found to show emission nebulosities in optical photographs (*e.g.* R Aqr). In view of the presence of a mass-losing cool star and a hot component supplying ionizing photons, symbiotic stars may generally be expected to have emission nebulosities around them. The ionized nebulae in most symbiotics are perhaps small in extent (compared with planetary nebulae). However, since the source of ionizing photons and the gas from the mass-losing cool star do not make a spherically symmetric system in the symbiotic binaries, one may expect, in addition to a compact ionized region, fainter extensions of

**Table 1.** Coordinates and other relevant information about the programme stars taken from Kenyon (1986).  $V$  and  $K$  are magnitudes in visual and infrared  $K$  passbands respectively. All the stars are variable in  $K$  magnitude.

Object	$\alpha_{1950}$			$\delta_{1950}$			$l$	$b$	Sp. type	$V$	$K$
	h	m	s	°	'	"					
H1-36	17	46	24.1	-37	00	36	353°.5	-4°.9	M	—	6.8
RR Tel	20	00	20.1	-55	52	04	342.2	32.2	M	14	3.6
R Aqr	23	41	14.3	-15	33	42	66.5	70.3	M7	5.8	-1.2

emission nebulosity in certain directions giving rise to bipolar (see *e.g.* Morris 1987) and other asymmetric structures that could be seen on deep photographs. Such extended nebulosities (ranging from 4–75 arcsec in angular size) were found in the symbiotic star He2-104 when CCD images in [O III] (Lutz 1988),  $H\alpha$ , [N II] and [S II] (Schwarz, Aspin & Lutz 1989) were taken. Emission-line CCD imaging of symbiotic stars may thus reveal the presence of extended nebulosities around other objects of this class.

Symbiotic stars that are more likely to show resolvable emission nebulosities are those that have large ionized regions. Such objects will also be relatively bright radio sources and thermal emission from the heated dust in the extended nebula will make them strong infrared sources. The dusty D-type symbiotics (*cf.* Webster & Allen, 1975; Allen 1982) that contain a Mira variable as the mass-losing cool component are therefore potential candidates for the detection of extended emission nebulosities. Therefore, we have selected R Aqr, RR Tel and H1-36 from the list of symbiotic stars given by Kenyon (1986) and have obtained CCD images through narrow-band filters centred at the emission lines of [O III],  $H\alpha$ , [N II] and [S II]. Table 1 lists the coordinates as well as other information about the objects under study.

## 2. Previous work

A brief description of the studies mainly carried out after 1984–85 on the objects under discussion is given below. Most of the work done prior to that has been elegantly summarized by Kenyon (1986).

R Aquarii being closest one (250 pc, according to Whitelock 1987), has attracted the attention of many investigators in recent years. A near UV optical map of the inner nebulosity taken with 1-arcsec resolution has been presented by Maun *et al.* (1985). The spectrum of R Aqr nebula has been studied by Wallerstein & Greenstein (1980). In order to study the structure and velocity field maps of the object, Solf & Ulrich (1985) and Hollis, Wagner & Oliverson (1990) have carried out its high resolution long-slit spectroscopy. Hollis, Wagner & Oliverson (1990) have also obtained a CCD image in the light of [O III]  $\lambda 5007$  and found evidence for a symmetrical jet structure in R Aqr. Multifrequency radio observations of R Aqr with the VLA were made by Hollis *et al.* (1985). A comparison of the 6 cm radio continuum structure with CCD imagery in  $H\alpha$  and  $H\beta$  has been done by Hollis, Oliverson & Wagner (1989). Using VLA data taken over a period of 5 years, Kafatos *et al.* (1989) have detected collimated 6 cm radio continuum emission southwest of R Aqr. In the infrared Schwarz *et al.* (1987) have

found spatially extended (over  $\sim 30$  arcsec) emission at  $3.45 \mu\text{m}$  with a morphology that is circularly symmetric about the central object.

To our knowledge, no emission-line imaging observations have been reported in the literature for RR Tel and H1-36. Taylor (1988) found the radio size of H1-36 to be  $\sim 0.6$  arcsec at  $\lambda = 2$  cm but observations at longer wavelengths reveal a more extended ( $\sim 5$  arcsec, see Table 1 in Taylor 1988) nebula.

### 3. Observations and reductions

The CCD images were obtained on two nights during 1989 June 23–25, with a blue-coated GEC Astromed Corp CCD detector at the  $f/8$  Cassegrain focus of the Australian National University 1.0 m telescope located at Siding Spring Observatory. The CCD of  $380 \times 576$  size has each pixel  $22 \mu\text{m}^2$  that corresponds to 0.56 arcsec on the sky and the total area covered by a CCD frame is  $\sim 3.54 \times 5.36$  square arcmin. The read-out noise for the system was about 7 electrons per pixel and the electrons per ADU was equal to 1. Flat field exposures ranging from 1 to 20 s in each filter were made of the twilight sky. Many short as well as long exposures for the programme stars were taken to detect the faint extended nebulosity without being completely swamped by the light of the central star. The details of these observations are given in Table 2. The exposure times were generally too short to saturate the CCD electronics. Only a few central pixels in the images of the stars were saturated in the case of the  $\text{H}\alpha$  300-s exposure for R Aqr and the  $\text{H}\alpha$  20- and 40-s exposures for RR Tel. The band widths (FWHM) were respectively 25, 50, 15 and  $50 \text{ \AA}$  for the [O III],  $\text{H}\alpha$ , [N II] and [S II] filters. It should be noted that due to the relatively large bandwidth of the  $\text{H}\alpha$  filter, the CCD images taken in this filter will be contaminated by [N II] emission.

The CCD data frames were corrected for bias and flat fields in the normal way using the FIGARO software at AAO, Epping. The evenness of the flat fields was better than 5–6 per cent in all the filters. Further data reductions were carried out using the computer facilities of the Astronomisches Institut der Universität, Bonn. The coloured pictures of the CCD images have been produced using the facilities available at MPIfR, Bonn.

**Table 2.** Details of observations.

Object	Filter	No. of frames	Exposure times (s)	Date	Seeing (arcsec)
RR Tel	[O III]	4	60, 120, 240, 300	1989 June 23/24	4.1
	$\text{H}\alpha$	3	10, 20, 40	"	3.9
	[N II]	4	60, 120, 240, 480	"	3.9
	[S II]	5	10, 60, 120, 240, 480	"	4.1
H1-36	[O III]	2	200, 600	1989 June 24/25	2.4
	$\text{H}\alpha$	3	60, 300, 600	"	1.8
	[N II]	2	300, 600	"	2.0
	[S II]	2	300, 900	"	1.8
R Aqr	[O III]	2	300, 600	"	$\sim 2$
	$\text{H}\alpha$	2	60, 300	"	"
	[N II]	1	300	"	"
	[S II]	1	300	"	"

#### 4. Results and discussion

##### 4.1 The Image Features of H1-36 and RR Tel

In each filter graded exposures have been taken (see Table 2). As the image features of an object in a filter are the same on different exposures, only one extracted image (size  $\sim 400 \times 270$  pixel<sup>2</sup>) in each filter is chosen for the illustration. In Figs 1 and 2, we present such coloured images for H1-36 and RR Tel respectively. Except a marginal circular asymmetry in the H $\alpha$  image of H1-36, no obvious nebulous features are seen in the images of these objects. Inspection of the H1-36 images in [S II] clearly indicates that the asymmetry in H $\alpha$  images is caused by a faint feature (most probably stellar type). As the source in H $\alpha$  is stronger than in [S II] (*cf* Allen 1983), its image has been merged with the faint feature in the H $\alpha$  CCD images.

To see whether the CCD emission-line images of H1-36 and RR Tel are extended or not, the following simple exercise was carried out.

(1) The standard width of the Gaussian stellar profile,  $\sigma$ , is estimated for all the CCD frames. This number has been used to get a quantitative estimate of the seeing for the CCD frame which is approximately equal to the full width at half maximum ( $2\sqrt{\ln(2)}\sigma = 2.355\sigma$ ) of the stellar core. The values of  $\sigma$  indicate that seeing was very poor ( $\sim 4$  arcsec) on the night of 1989 June 23/24 and was somewhat better ( $\sim 2$  arcsec) on the night of 1989 June 24/25.

(2) The values of  $\sigma$  are also estimated for RR Tel and H1-36 on each CCD image. A comparison of these with the corresponding values of  $\sigma$  derived from stellar images show that there is no statistical difference between them.

This leads us to conclude that for RR Tel and H1-36 size of the emission nebulosity in the optical region is less than the values of seeing *i.e.* 4 and 2 arcsec respectively on their observing nights. These objects do not have extended and bright emission nebulous features like those present in He2-104 and R Aqr, otherwise they would have been seen even in the present poor spatial resolution. In R Aqr we have detected a faint nebulosity (see Figs 3 and 4) in H $\alpha$  at an angular distance as large as 70 arcsec from the centre with an exposure time of 300 s. No extended emission beyond the seeing scale was found in H1-36 frames taken on the same night with exposure times longer by a factor of 2 in H $\alpha$  and [N II] and by a factor 3 in [S II].

Any nebulosity in the optical emission lines in H1-36 must be smaller than  $\sim 2$  arcsec. In R Aqr, on the other hand, the optical nebulosity is much larger ( $\sim 2$  arcmin).

RR Tel also has not shown any extended nebulosity in the CCD images. The radio size of RR Tel is not known. It should be noticed that both H1-36 and RR Tel are brighter than R Aqr in radio. The radio flux densities for these three objects at 4.9 GHz are 46 mJ, 28 mJ and 12 mJ respectively (*cf*. Seaquist 1988) and their radio spectra are similar, their spectral indices being 1.0, 0.52 and 0.60 respectively (*cf*. Kenyon 1986). The radio size is positively correlated with the radio flux density for physically similar sources (*cf* Taylor 1988) and the optical nebulosity which is caused by optical recombination-line emission is expected to be at least as large as the radio-emitting H II region. Therefore H1-36 and RR Tel are also expected to have extended optical nebulosities with sizes  $\sim 10$  arcsec, just as R Aqr. The non-detection of optical nebulosity around H1-36 and RR Tel is therefore puzzling. While the seeing during the

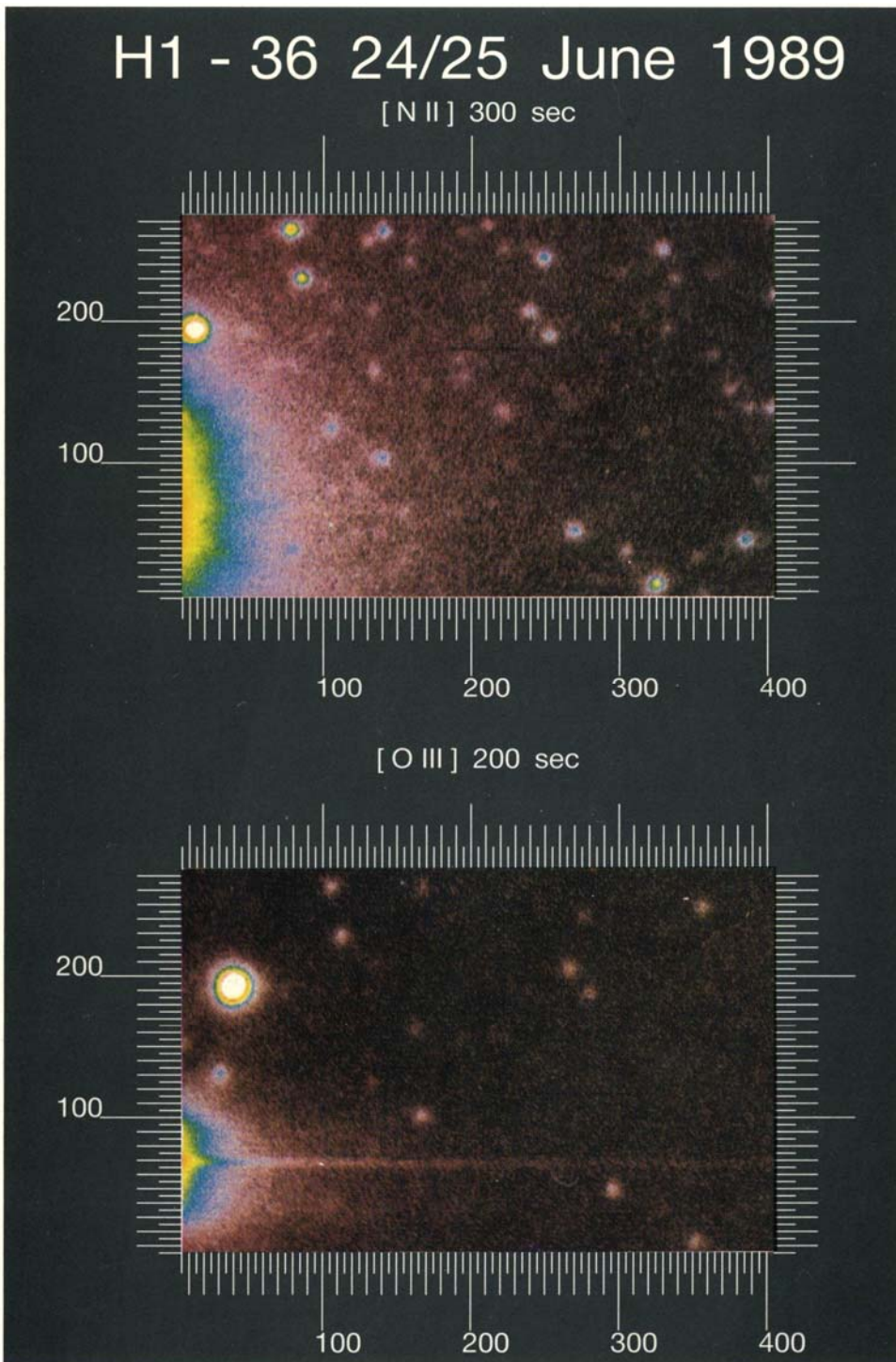
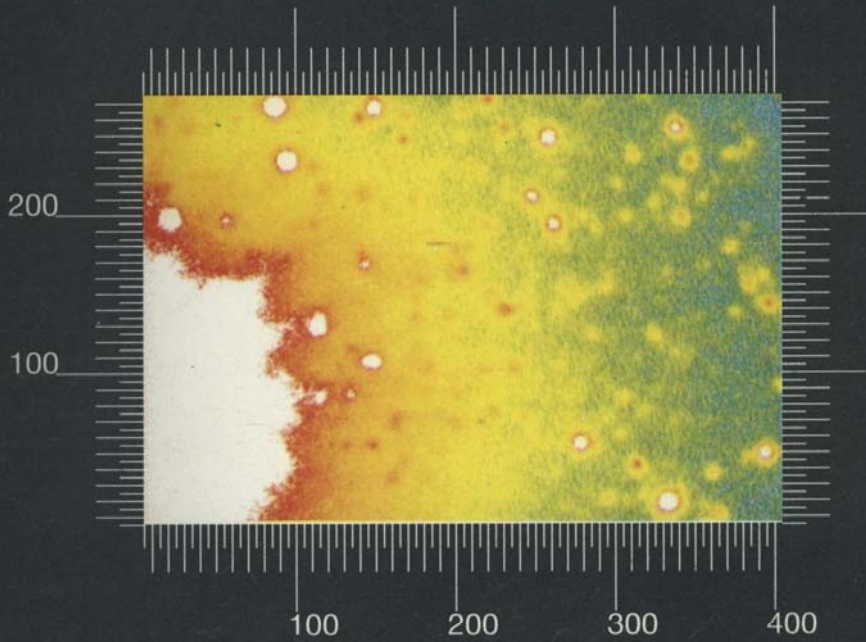


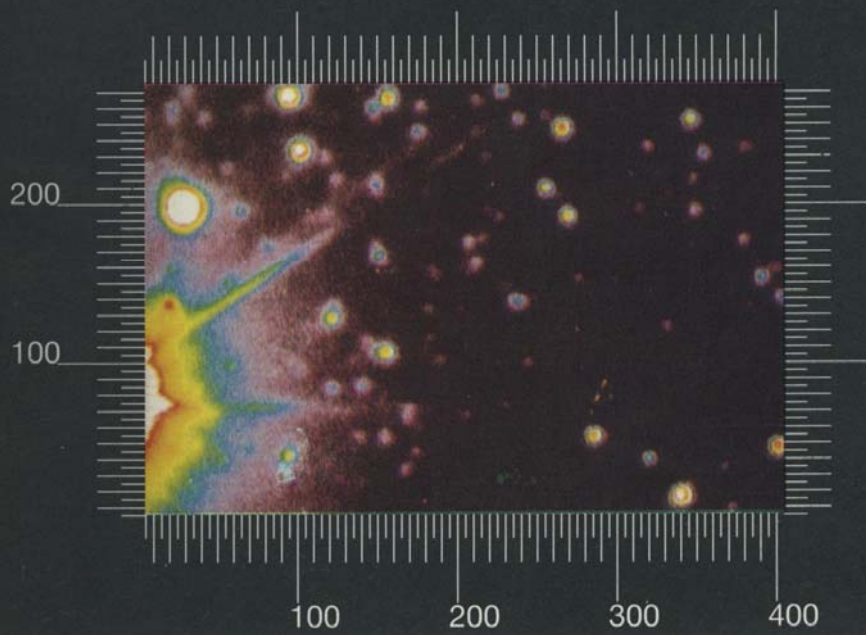
**Figure 1.** Colour map of H1-36 region. The H1-36 is the brightest object seen in [O III] image. North is upward and east is to the left. The coordinates are in pixels. Exposure times in seconds are written after the filter name.

H.C. BHATT & RAM SAGAR

[ S II ] 300 sec



H alpha 600 sec



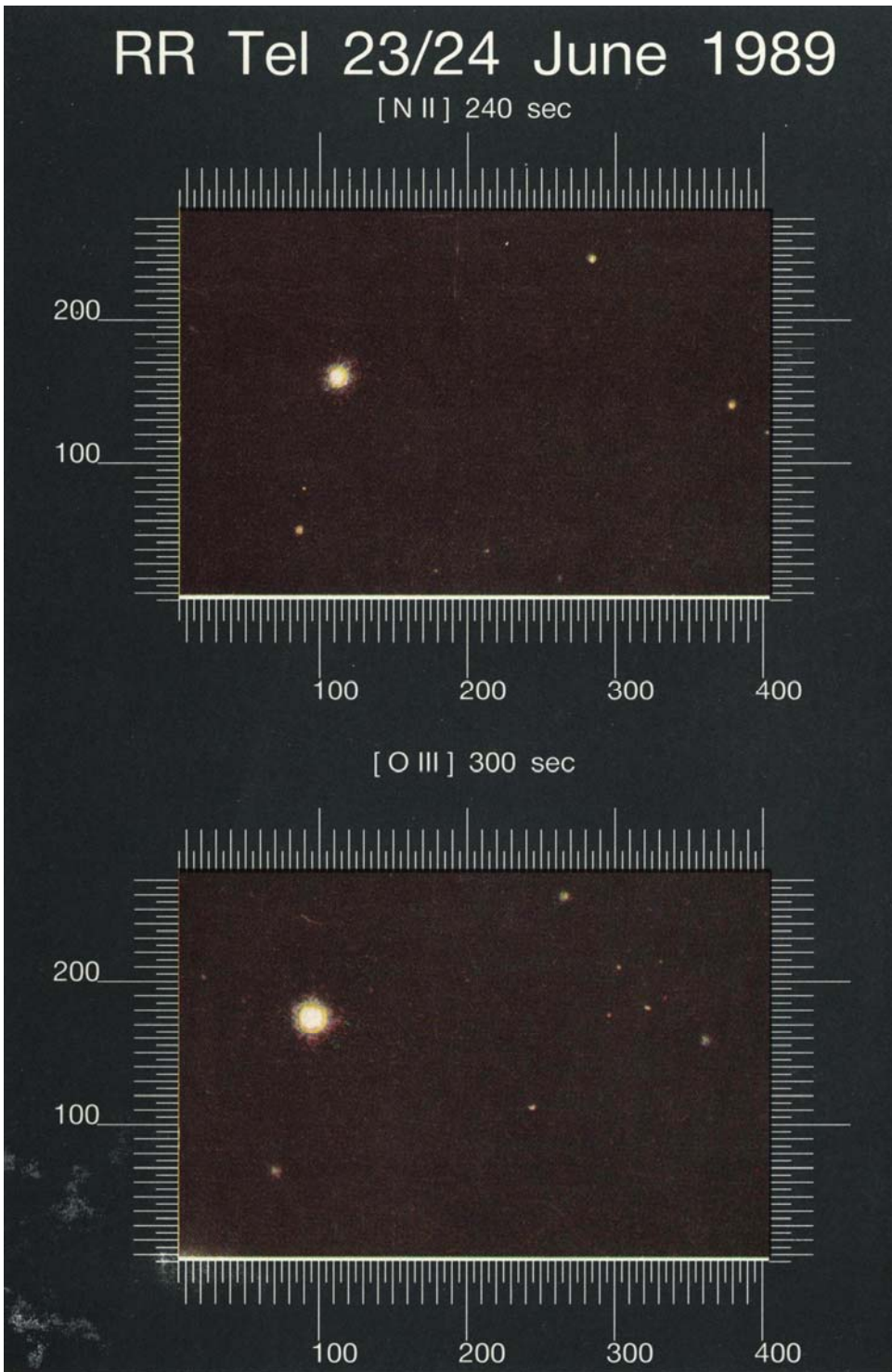
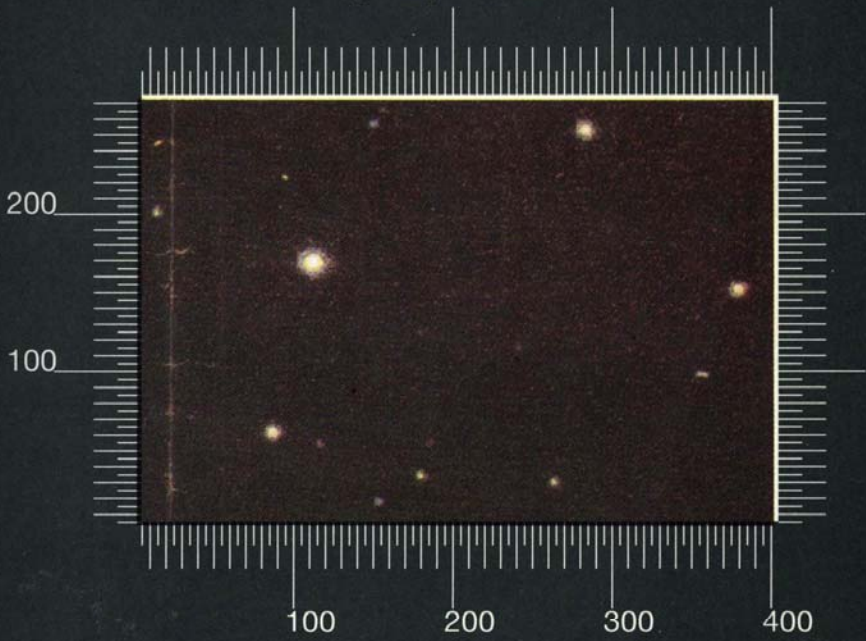


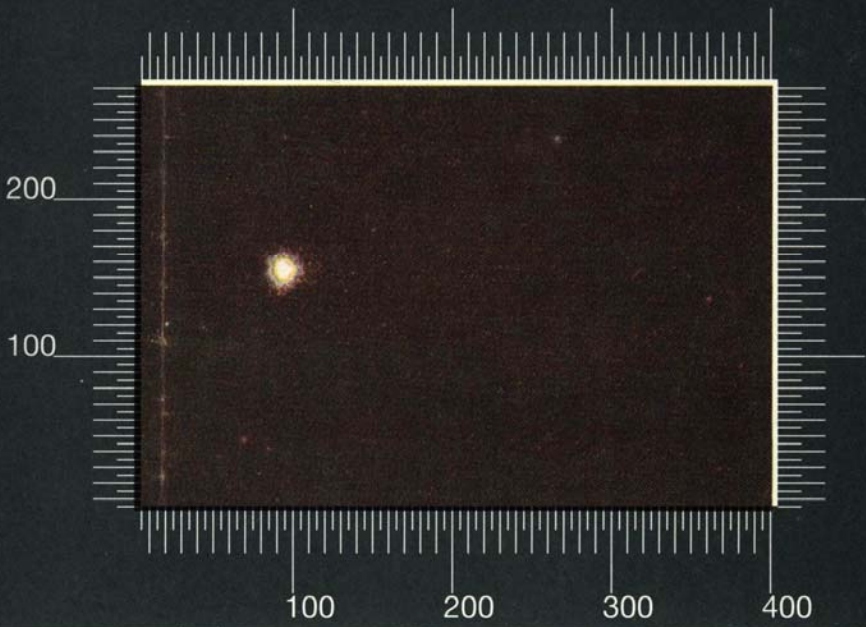
**Figure 2.** Colour map of the region around RR Tel. The brightest object in the field is RR Tel. Orientation and other notations are the same as in Fig. 1.

H.C. BHATT & RAM SAGAR

[ S II ] 480 sec



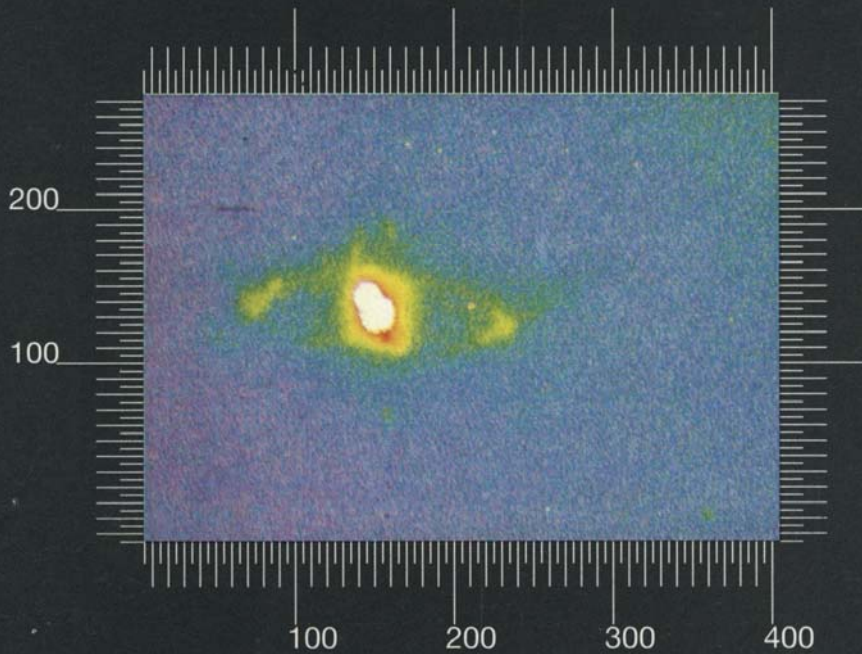
H alpha 10 sec





R Aqr 24/25 June 1989

[ N II ] 300 sec



[ O III ] 300 sec

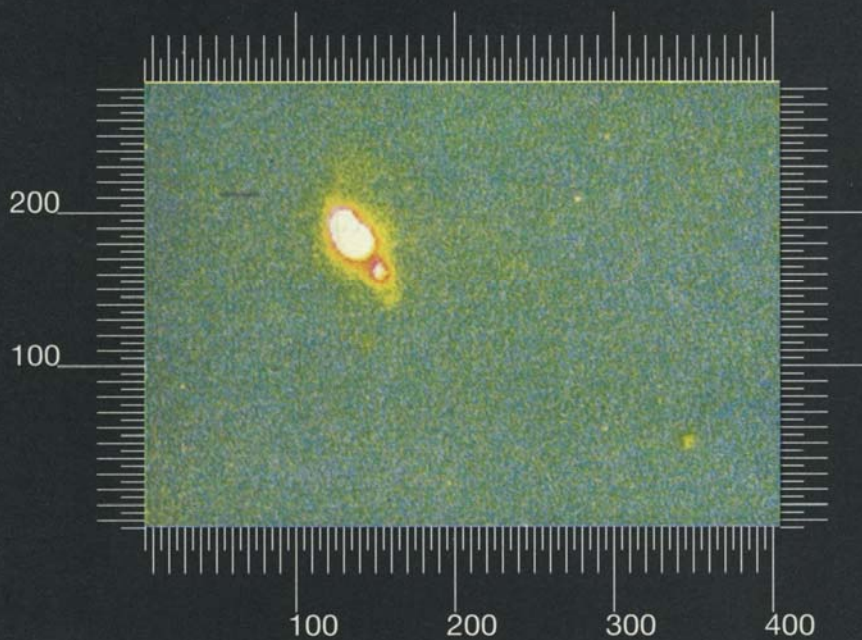
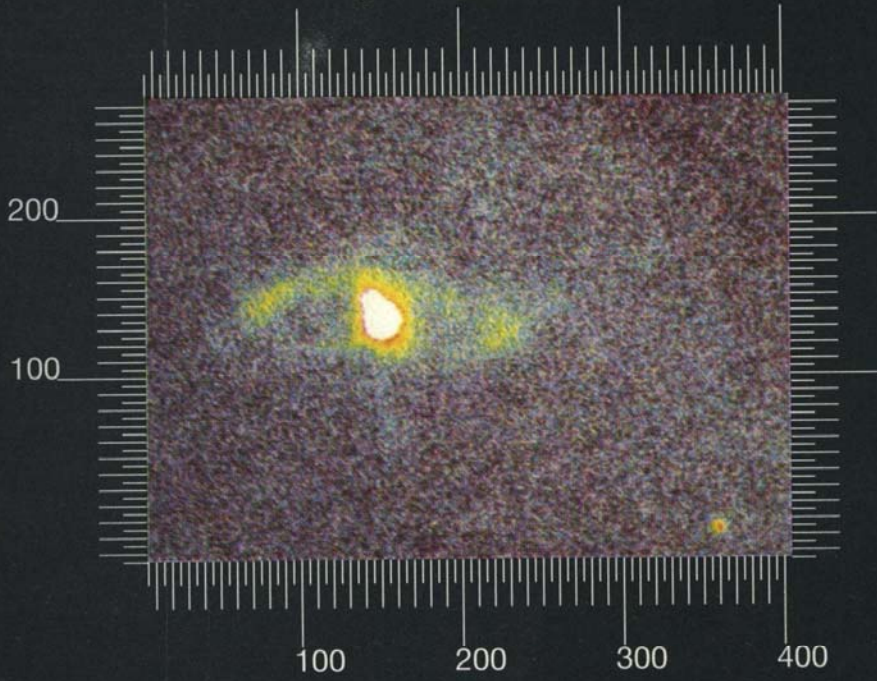


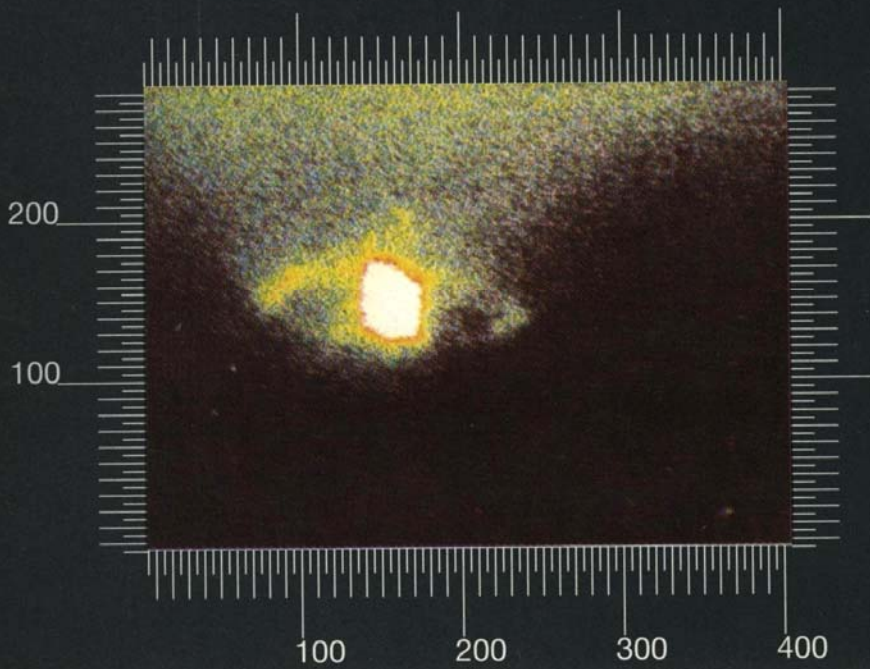
**Figure 3.** Colour picture of the faint nebulous features of R Aqr. Orientation and other notations are the same as in Fig. 1.

H.C. BHATT & RAM SAGAR

[S II] 300 sec



H alpha 300 sec



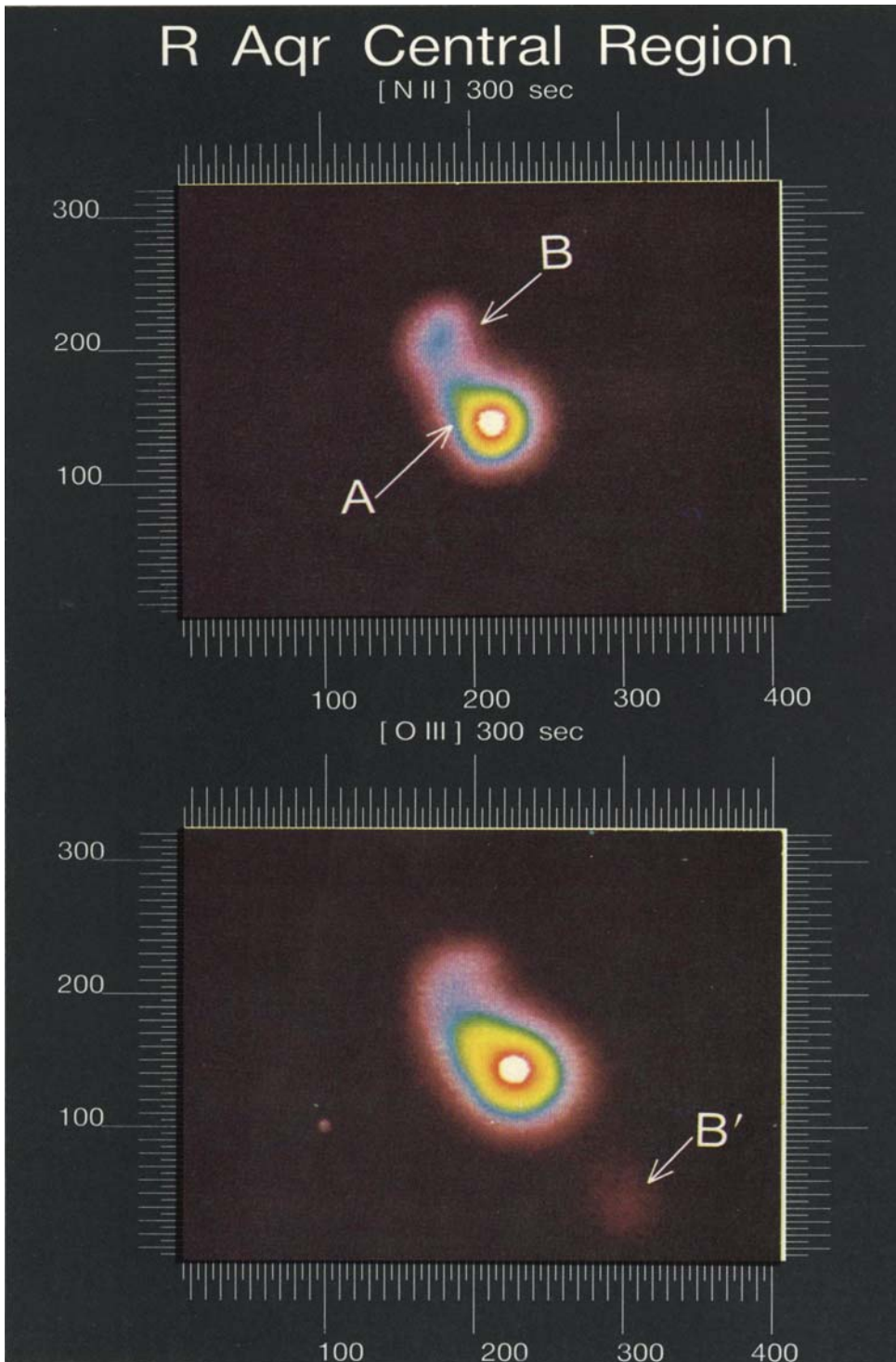
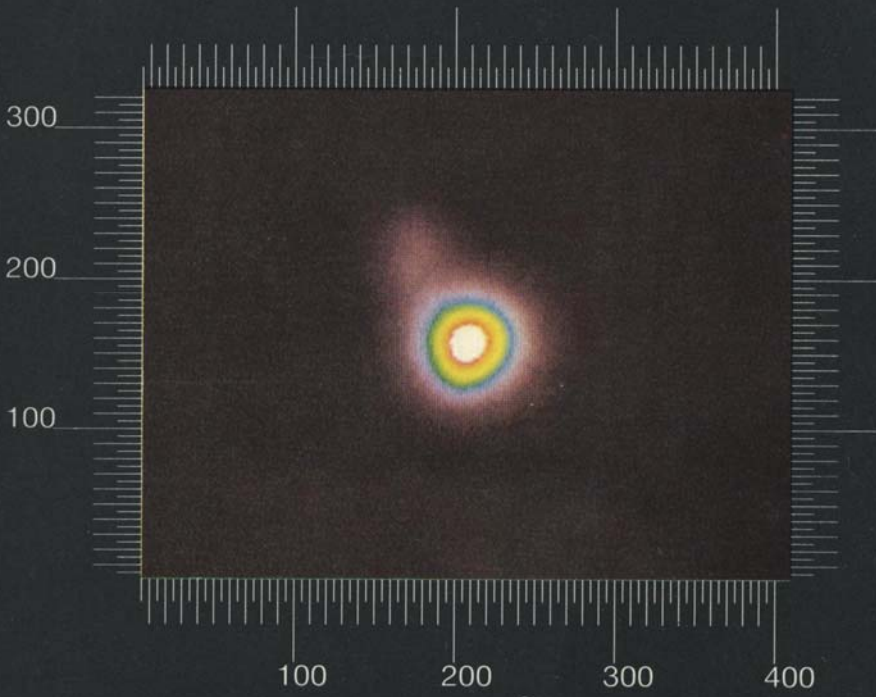
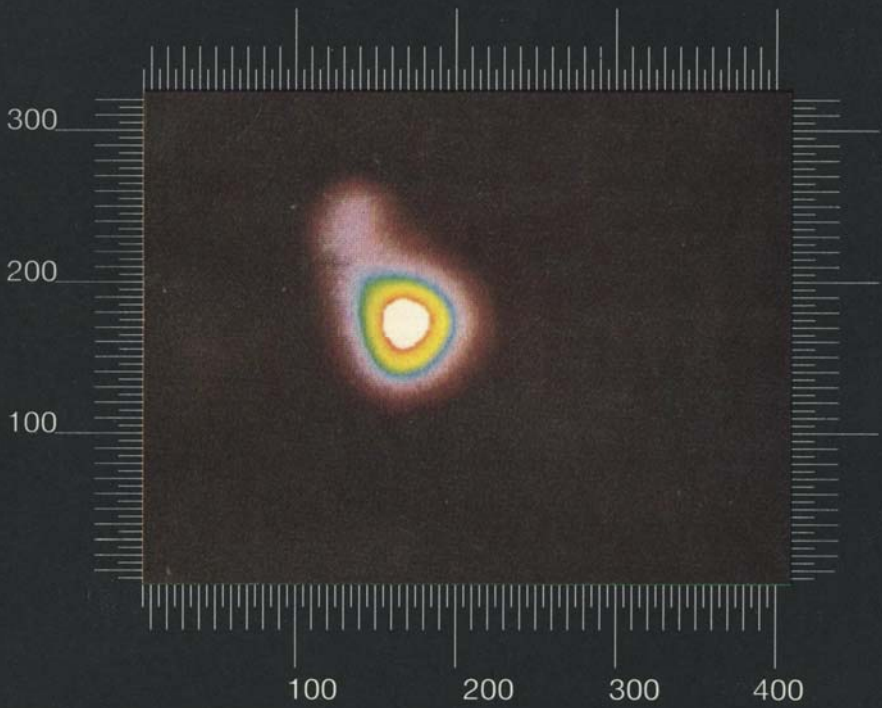


**Figure 4.** Colour picture of the central region of R Aqr. The images have been magnified 4 times. Orientation and other notations are the same as in Fig. 1. However, as a result of magnification, 4 pixels of the image correspond to one pixel in Fig. 3. The features A, B' (see text) have been labeled.

[ SII ] 300 sec



H alpha 300 sec



observations of RR Tel was rather poor ( $\sim 4$  arcsec) and almost comparable to the expected radio size, the object H1-36 was observed on the same night as R Aqr when the seeing was  $\sim 2$  arcsec. Interstellar extinction may be responsible for the non-detection of optical nebulosities. We think that this is the case for H1-36 which is the closest, of the three objects, to the Galactic plane (galactic latitude  $b = -4^\circ.9$ , see Table 1), is in the direction of Galactic Centre (galactic longitude  $l = 353^\circ.5$ ), and is probably a distant object ( $\sim 4\text{--}5$  kpc, Allen 1983). R Aqr, on the other hand, is a nearby (250 pc, Whitelock 1987) high galactic latitude object suffering very little interstellar extinction. The galactic latitude of RR Tel ( $b = 32^\circ.2$ ) is also high, but it does not show any extended optical nebulosity on a scale like that of R Aqr. It is possible that circumstellar extinction due to dust in the stellar wind from the cool component suppresses optical emission from the ionized regions in some symbiotic systems. Also, the radio size of a nebula depends on the radio frequency used and the density structure, so that for a centrally condensed nebula the optical emission comes from a compact core while in radio the tenuous outer regions may show up as extended structures. The differences in the circumstellar environs can thus cause differences in the observed nebulous features.

#### 4.2 The Nebulous Features of R Aqr

The nebulosity around R Aqr is presently known to be comprised of at least three different structures. First, the 2 arcmin outer nebula shows filamentary structure and has a more compact central part surrounded by an elongated elliptical ring in the direction of right ascension. Second, a 1 arcmin inner structure is centred on R Aqr, is elongated in declination, and is perpendicular to the orientation of the outer nebulosity. These two features have been known for a long time (Lampland 1922). Third, a central H II region is associated with the inner nebulosity. This has been recently discovered and seen best at the radio wavelengths (see Hollis, Oliverson & Wagner 1989 and references therein). It has several discrete features protruding along a curve extending from the central H II region toward the north east for  $\sim 10$  arcsec.

The CCD images presented here are through narrow-band filters at the wavelengths of the high-excitation line of [O III] as well as H $\alpha$  and the low-excitation lines of [N II] and [S II]. Fig. 3 shows the faint nebulous features of R Aqr images. The count levels used to display the pictures are listed in Table 3. The image regions having counts above the maximum level used in the display are white in colour and occupy the

**Table 3.** Photon levels used to display the colour image of R Aqr.

Filter	Photon counts used for displaying image features in			
	Figure 3		Figure 4	
	minimum	maximum	minimum	maximum
[O III]	50	225	150	7,000
H $\alpha$	960	1150	1150	50,000
[N II]	60	350	200	12,000
[S II]	370	540	350	12,000

central part of the nebula. Fig. 3 shows extensive structural detail. The faint image features of R Aqr in [N II] and [S II] are more or less similar to those in  $H\alpha$ , but they are very different in [O III]. We note the following points.

(i) The elliptical outer ring in the direction of right ascension is seen in the low excitation lines of [N II] and [S II] and  $H\alpha$  only. It is not seen in the high excitation line of [O III].

(ii) In order to see the image features in the central region of R Aqr, we present its 4 times magnified coloured map in Fig. 3. The original size of the area used in Fig. 4 is  $\sim 100 \times 80$  pixel<sup>2</sup>. The count levels used to display the colour are given in Table 3. The colour of the central region of the R Aqr in all the filters is white because the number of photons in that area are more than the maximum level of the counts used to display the colour. The number of counts decreases as one moves away from the centre. The different colours effectively indicate the various relative intensity levels. Image features differ remarkably from one filter to other. In the discussion to follow, we have used the nomenclature given by Kafatos *et al.* (1989) for the image features. The feature B is present in all the images while the feature B' is seen only in the [O III] image. The relative intensity distribution between the feature B and the central star is quite different in different filters. The asymmetry (seen in yellow and blue colours) present toward the northeast side in the images of [O III],  $H\alpha$  and [N II] is most probably due to the feature A. This feature seems to be very weak in [S II] because the image of the central star is almost circular. The features A and B have also been seen in UV light by Mauron *et al.* (1985). Because of the relatively poor resolution ( $\sim 2$  arcsec) of the present CCD images, it is not possible to identify the other features seen close to the central source in the high resolution radio map of Kafatos *et al.* (1989).

(iii) The symmetrical jet like structure is clearly seen only in [O III]. It is not apparent in  $H\alpha$ , [N II] and [S II].

(iv) The radio maps of R Aqr given by Sopka *et al.* (1982), Hollis *et al.* (1985), Kafatos, Hollis & Michalitsianos (1983), Kafatos *et al.* (1989) as well as the UV map presented by Mauron *et al.* (1985) resemble the [O III] image.

The above discussion leads us to conclude that the nebula in R Aqr is ionization-stratified. The [O III] emission comes from the central region that is coincident with the radio emitting region. The central core may be a radiation bounded ionized region that is optically thick. High energy photons that can ionize  $O^+$  are not able to escape this region and produce [O III] emission in the outer elliptical rings. Perhaps no ionization is taking place in the 2 arcmin outer elliptical ring and it may be a fossil H II region produced about  $\sim 10^3$  yr ago when it was ejected from the central source (Baade 1943). It is now simply going through the process of recombination and cooling.

## 5. Conclusion

CCD imaging of D-type symbiotics R Aqr, RR Tel and H1-36 has been carried out in narrow-band filters centred at the emission lines of [O III],  $H\alpha$ , [N II] and [S II]. No bright and extended emission nebulosities like those observed in He2-104 (*cf.* Lutz 1988; Schwarz *et al.* 1987) and R Aqr were detected in RR Tel and H1-36. Size of the inner emission nebulosities may be smaller than  $\sim 4$  arcsec in RR Tel and  $\sim 2$  arcsec in

H1-36. In the case of H1-36 which is known to have a radio image size of  $\sim 5$  arcsec, interstellar and/or circumstellar extinctions may be responsible for the non-detection of emission nebulosity. If very faint nebulosities exist in these systems, they will need better resolution and much longer exposures. The R Aqr nebulosity shows ionization-stratification. The 2 arcmin and 1 arcmin outer elliptical rings in R Aqr are seen in  $H\alpha$  and in the low-excitation lines of [N II] and [S II] while the high excitation [O III] emission comes only from the central bipolar region that is coincident with the radio and UV emitting region. The symmetrical jet-like structure is clearly seen only in [O III]. The outer elliptical ring in R Aqr may be a fossil H II region produced  $\sim 10^3$  yr ago when it was ejected from the central source.

### Acknowledgements

We thank the Director of Mount Stromlo Observatory for allotment of telescope time. We are thankful to Prof. Dr. K. S. de Boer, Prof. H. Schwarz and referees for the useful comments on the manuscript. RS gratefully acknowledges the support from the Department of Industry, Technology, and Commerce of Australia and the IAU for a visit to Australia. He also thanks the Alexander von Humboldt Foundation for a research fellowship to work in Bonn.

### References

- Allen, D. A. 1982, in *IAU Coll. 70: The Nature of Symbiotic stars*, Eds M. Friedjung & R. Viotti, D. Reidel, Dordrecht, p. 27.
- Allen, D. A. 1983, *Mon. Not. R. astr. Soc.*, **204**, 113.
- Baade, W. 1943, *Ann. Rep. of the Director of Mount Wilson Obs. 1943–44*, p. 12.
- Hollis, J. M., Oliverson, R. J., Wagner, R. M. 1989, *Astrophys. J.*, **337**, 795.
- Hollis, J. M., Kafatos, M., Michalitsianos, A. G., McAlister, H. A. 1985, *Astrophys. J.*, **289**, 795.
- Hollis, J. M., Wagner, R. M., Oliverson, R. J. 1990, *Astrophys. J.*, **351**, L17.
- Kafatos, M., Hollis, J. M., Michalitsianos, A. G. 1983, *Astrophys. J.*, **267**, L103.
- Kafatos, M., Hollis, J. M., Yusef-Zadeh, F., Michalitsianos, A. G., Elitzur, M. 1989, *Astrophys. J.*, **346**, 991.
- Kenyon, S. J., 1986, *The Symbiotic Stars*, Cambridge Univ. Press, Cambridge.
- Lampland, C. O. 1922, *Pop. Astr.*, **30**, 618.
- Lutz, J. H., 1988, in *Proc. IAU Coll. 103: The Symbiotic Phenomenon*, Eds J. Mikolajewska, M. Friedjung, S. J. Kenyon & R. Viotti, Kluwer, Dordrecht, p. 305.
- Mauron, N., Nieto, J. L., Picat, J. P., Lelievre, G., Sol, H. 1985, *Astr. Astrophys.*, **142**, L13.
- Morris, M. 1987, *Publ. astr. Soc. Pacific*, **99**, 1115.
- Seaquist, E. R. 1988 in *IAU Coll. 103: The Symbiotic Phenomenon*, Eds J. Mikolajewska, M. Friedjung, S. J. Kenyon & R. Viotti, Kluwer, Dordrecht, p. 69.
- Schwarz, H. E., Aspin, C., Lutz, J. H. 1989, *Astrophys. J.*, **344**, L29.
- Schwarz, H. E., Aspin, C., Lutz, Hanner, M., Zarnecki, J. 1987, in *Infrared Astronomy with Arrays*, Eds C. G. Wynn-Williams & E. E. Becklin, Univ. Hawaii, Institute for Astronomy, Honolulu, p. 312.
- Solf, J., Ulrich, H. 1985, *Astr. Astrophys.*, **148**, 274.
- Sopka, R. J., Herbig, G., Kafatos, M., Michalitsianos, A. G. 1982, *Astrophys. J.*, **258**, L35.
- Taylor, A. R. 1988 in *IAU Coll. 103: The Symbiotic Phenomenon*, Eds J. Mikolajewska, M. Friedjung, S. J. Kenyon, R. Viotti, Kluwer, Dordrecht, p. 77.
- Wallerstein, G., Greenstein, J. L. 1980, *Publ. astr. Soc. Pacific*, **92**, 275.
- Webster, B. L., Allen, D. A. 1975, *Mon. Not. R. astr. Soc.*, **171**, 171.
- Whitelock, P. A. 1987, *Publ. astr. Soc. Pacific*, **99**, 573.